

Varved sediment responses to early Holocene climate and environmental changes in Lake Meerfelder Maar (Germany) obtained from multivariate analyses of micro X-ray fluorescence core scanning data

Martin-Puertas, Celia; Tjallingii, Rik; Bloemsma, Menno; Brauer, Achim

DOI

[10.1002/jqs.2935](https://doi.org/10.1002/jqs.2935)

Publication date

2017

Document Version

Final published version

Published in

Journal of Quaternary Science

Citation (APA)

Martin-Puertas, C., Tjallingii, R., Bloemsma, M., & Brauer, A. (2017). Varved sediment responses to early Holocene climate and environmental changes in Lake Meerfelder Maar (Germany) obtained from multivariate analyses of micro X-ray fluorescence core scanning data. *Journal of Quaternary Science*, 32(3), 427-436. <https://doi.org/10.1002/jqs.2935>

Important note

To cite this publication, please use the final published version (if applicable). Please check the document version above.

Copyright

Other than for strictly personal use, it is not permitted to download, forward or distribute the text or part of it, without the consent of the author(s) and/or copyright holder(s), unless the work is under an open content license such as Creative Commons.

Takedown policy

Please contact us and provide details if you believe this document breaches copyrights. We will remove access to the work immediately and investigate your claim.

Varved sediment responses to early Holocene climate and environmental changes in Lake Meerfelder Maar (Germany) obtained from multivariate analyses of micro X-ray fluorescence core scanning data

CELIA MARTIN-PUERTAS,^{1,2*} RIK TJALLINGII,^{1*} MENNO BLOEMSMA^{3,4} and ACHIM BRAUER¹

¹GFZ-German Research Centre for Geosciences, Section 5.2 Climate Dynamics and Landscape Evolution, Telegrafenberg, Potsdam D-14473, Germany

²Department of Geography, Royal Holloway, University of London, Egham, Surrey TW20 0EX, UK

³Delft University of Technology, Faculty of Civil Engineering and Geosciences, Department of Geotechnology, Stevinweg 1, NL-2628CN Delft, The Netherlands

⁴Tata Steel – Netherlands Main Office, Postbus 10000, 1970 CA IJmuiden, The Netherlands

Received 25 May 2016; Revised 25 November 2016; Accepted 9 January 2017

ABSTRACT: We present an early Holocene record from Lake Meerfelder Maar in Germany for in-depth interpretation of depositional changes in annually laminated lake sediments as proxies for climatic and local environmental changes. We characterized the compositional changes in the sediment record using Ward's clustering analyses of the micro X-ray fluorescence core scanning data and linked these to microfacies descriptions. The down-core distribution of the clusters allowed us to define boundaries that represent variations of a comprehensive element assemblage occurring at 11 555, 11 230, 10 650, 10 515 and 9670 varve a BP. Our main results show that during the Early Holocene the long-term vegetation reorganization and evolution of the lake's catchment played a predominant role for sediment deposition. Abrupt shifts occurred at the Younger Dryas/Holocene and the Preboreal/Boreal biostratigraphical boundaries. We do not observe clear signals corresponding to known short-term climatic oscillations described in the North Atlantic region such as the Preboreal Oscillation. A unique and intriguing episode in the history of the lake of predominantly organic deposition and very low amounts of allochthonous sediments occurred between 10 515 and 9670 varve a BP and is related to hydrological thresholds. Copyright © 2017 John Wiley & Sons, Ltd.

KEYWORDS: central Europe; clustering of μ -XRF core scanning data; early Holocene; varved lake sediments.

Introduction

Annually laminated (varved) lake sediments provide continuous information of climate change and landscape evolution in the human habitat. These sediment records allow the study of both long-term and abrupt climatic changes with seasonal time resolution before the instrumental period (Brauer *et al.*, 1999; Martin-Puertas *et al.*, 2012a,b; Czymzik *et al.*, 2013). The most recent techniques for the study of varved records include parallel investigation of microfacies analyses and geochemical information derived from micro X-ray fluorescence (μ -XRF) core scanning data (Dulski *et al.*, 2015). This approach improves the interpretation of the observed chemical signals because those can be directly compared to observations of microfacies changes, which provide a better description of the sediments. However, characterization of sedimentological changes using single elements might give a simplistic interpretation of the climatic and environmental processes, as these changes are often related to variations in element assemblages (Bloemsma *et al.*, 2012). So, studying variability of element assemblages rather than single elements can provide a better understanding of lake sedimentation and particularly of the mechanisms of varve formation. By adopting this novel approach it will be possible to objectively distinguish even more subtle geochemical changes in the sediment record

that would remain undetected by conventional analyses, as well as to establish if the control on sedimentation patterns is driven by land cover changes induced by either natural vegetation succession or short-lived climatic events.

During the transition into the present interglacial conditions between 11 590 and 9000 a BP, the climatic and environmental conditions in central Europe were characterized by large climatic re-organizations that were regionally differently influenced by the progressive melting of the Fennoscandian ice sheet and rising sea level, including flooding of the North Sea basin (Björck, 2008). Northern Hemisphere air temperature variability reconstructed from $\delta^{18}\text{O}$ isotope records in Greenland (Masson-Delmotte *et al.*, 2005; Rasmussen *et al.*, 2014) and in central Europe (von Grafenstein *et al.*, 1999) shows an initial abrupt warming followed by a further gradual temperature increase. This resulted in a rapid shift from the cold continental conditions of the Younger Dryas (YD) to temperate climate with milder winters and warmer summers in central Europe (Renssen, 2001). Short-lived synchronous $\delta^{18}\text{O}$ anomalies in the Greenland ice cores are superimposed on this multi-centennial timescales trend at 11.4, 10.3 and 9.3 ka b2k (Rasmussen *et al.*, 2014). These rapid isotope excursions have been related to cool pulses in the North Atlantic realm, i.e. the so-called 'Preboreal Oscillation' (PBO), 'Boreal Oscillation' (BO) and the '9.3 ka event', respectively (e.g. Björck *et al.*, 1997; McDermott *et al.*, 2001; Wohlfarth *et al.*, 2007; Bos *et al.*, 2007; Lauterbach *et al.*, 2011).

*Correspondence to: Celia Martin-Puertas or Rik Tjallingii.
E-mails: celia.martinpuertas@rhu.ac.uk, rik.tjallingii@gfz-potsdam.de

In northern and central Europe, the most significant environmental responses at the transition to interglacial conditions were the re-forestation through a plant succession influenced not only by climate but also by re-immigration of species from their glacial refugia in southern Europe and soil formation. The initial phase of the Holocene was still dominated by *Betula* and *Pinus* (Preboreal period in the Blytt-Sernander classification) and followed by an expansion of *Corylus* (Boreal period) (Litt *et al.*, 2009; Theuerkauf *et al.*, 2014). In northern–central Europe, short-term interruptions of forest development have been reported to coincide with the rapid cold oscillations, especially the ‘PBO’ (Björck *et al.*, 1997; Bos *et al.*, 2007).

The pollen record from the varved sediments of Lake Meerfelder Maar (MFM, Germany) captures the vegetation succession described in central Europe throughout the Early Holocene at 20–100 years resolution (Litt *et al.*, 2009) but does not record the short-term fluctuations. These pollen data can be directly compared to our seasonally resolved sediment proxies from MFM, giving the opportunity to study differences and similarities between the vegetation and lake responses to shifting environmental and climatic conditions. Previous studies on the MFM sediments link changes in varve thickness and composition to large-scale climatic changes such as the onset and termination of the YD (Brauer *et al.*, 1999), but also lower amplitude fluctuations during the Late Holocene such as the ‘2.8 ka oscillation’ (Martin-Puertas *et al.*, 2012a). For the Early Holocene, the climatic signal in the MFM sediments is, however, remains of debate (Martín-Puertas *et al.*, 2012b).

Here, we test advanced clustering for the total μ -XRF core scanning dataset as a suitable tool to better depict environmental and climatic changes in the geochemical record. Our specific objective is to investigate to what extent changes in sediment deposition respond to either the long-term changes of the surface conditions in the catchment and/or short-term climatic oscillations.

Study site

MFM is located in the Westeifel Volcanic Field, Germany (50° 06'N, 6°45'E). The lake is within a steep-sided volcanic crater, where the crater walls have a relief of 170 m. The lake is located at 336.5 m a.s.l., and has a water depth of up to 18 m. The modern lake surface area is 0.248 km², covering the northern part (about one-third) of the maar crater area (Fig. 1). The southern part is formed by a shallow delta plain, deposited during the last glacial period by the Meerbach stream that entered the crater from the south (Brauer *et al.*, 1999). In historical times, the course of this stream has been changed several times for water regulation purposes. Today, it passes the crater south of the lake and exits the crater through a narrow gorge in the south-east (Fig. 1). The modern catchment is formed only of the crater (1.52 km²) but the catchment has been almost four times larger (5.76 km²) in the past, when the Meerbach stream still discharged into the lake. The course of this stream has great influence on the water balance and the sediment supply to the lake (Negendank *et al.*, 1990). Due to the morphology of the crater, a rise in lake level of only 2 or 3 m would result in a three times larger lake surface, by flooding most of the southern delta plain and creating a large shallow-water area (Brauer *et al.*, 1999). Past lake level changes have been identified by former lake terraces, which, however, are of unknown age (Negendank *et al.*, 1990). Due to its particular morphological situation in a deep maar crater (Fig. 1), MFM is wind-sheltered favouring the preservation of fine seasonal layers within the sediment sequence. There is a hiatus of only ca. 240 varve years, which was recognized by microscopic investigation at ca. 9700 varve a BP (Brauer *et al.*, 2000).

The temperate climate of the region is influenced by the Atlantic Ocean. Present-day temperature varies from -0.3° C (mean winter air temperature) to 16.3° C (mean summer air temperature). Mean annual precipitation is 950 mm, which

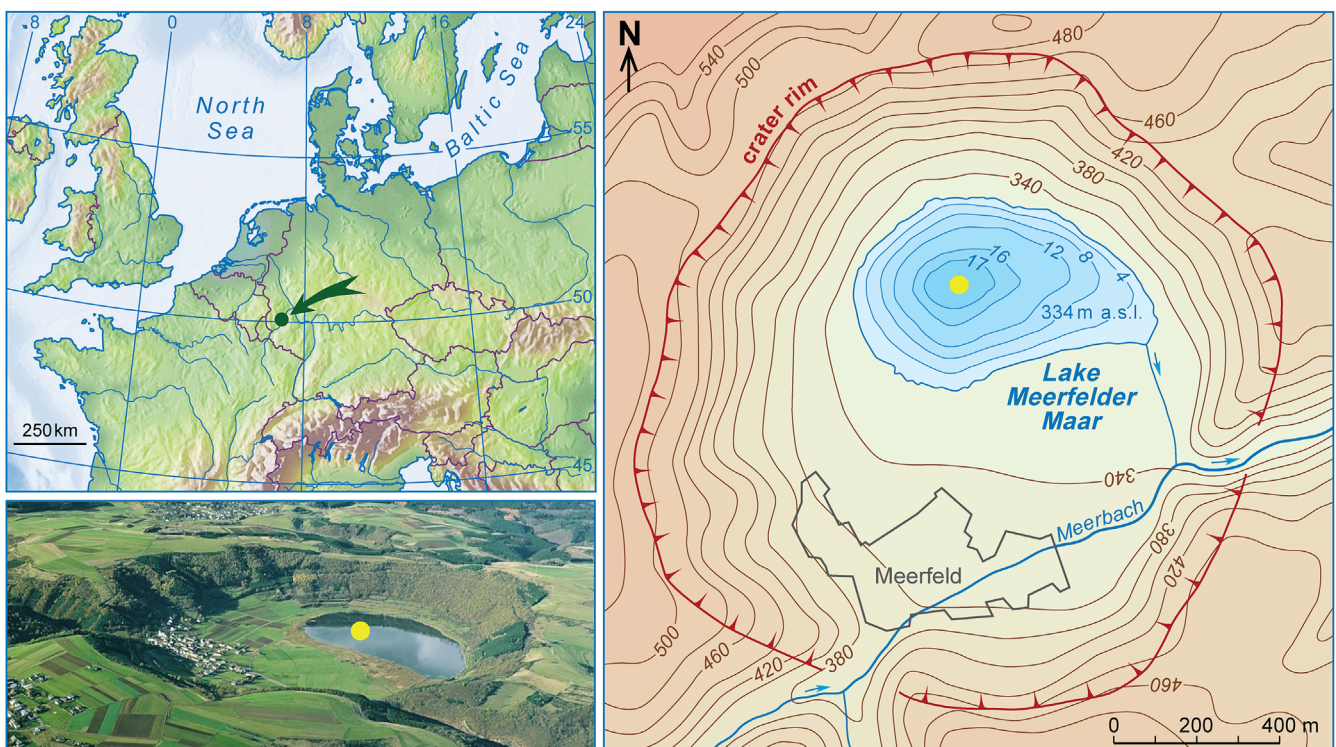


Figure 1. Maps and aerial photo of Lake Meerfelder Maar indicating topography of the crater, the bathymetry of the lake and the locations of the coring sites (yellow circle).

reaches the highest monthly values in winter (Litt *et al.*, 2009).

Materials and methods

In this study we use sediment cores collected during two coring campaigns in 1996 (MFM6) and 2009 (MFM09). The MFM6 cores have been obtained with a Usinger piston-coring device (Brauer *et al.*, 1999), while the MFM09 cores were recovered using a UWITEC piston corer (Martín-Puertas *et al.*, 2012b). The 11.20-m-long MFM6 composite profile was composed of five individual core sequences (Brauer *et al.*, 2000), while the 11.71-m-long MFM09 composite profile was made combining two core sequences (MFM09-A and MFM09-D). All cores from both MFM6 and MFM09 composite profiles were correlated using macro- and microscopic layers (Table 1; Fig. 2).

Varve counting and detailed thickness measurements for each individual varve were carried out on thin sections (120 × 35 mm), with a 2-cm overlap, using a petrographic microscope under plane and cross polarized light (magnification 100×) (Brauer *et al.*, 1999).

μ -XRF core scanning and multivariate analyses

We used the cores recovered in 2009 to analyse the chemical sediment composition of MFM. Measurements were carried out at 0.2-mm resolution with the ITRAX μ -XRF-core scanner at GFZ-Potsdam, Germany (Martín-Puertas *et al.*, 2012b). The high-resolution measurements provide 1–16 geochemical data points per varve depending on the annual sedimentation rate (varve thickness). The μ -XRF core scanner irradiated the split core surface with a molybdenum X-ray source for 20 s, operated at 30 kV and 40 mA, generating energy dispersive XRF radiation. In this way, the element intensities of Si, K, Ca, Ti, Mn, Fe, Ni, Rb, Sr and Zr as well as relative variations of the coherent and incoherent radiation were acquired non-destructively. The measured chemical composition of the sediment is expressed as element intensities (c.p.s.), which are non-linearly correlated to element concentration due to changing matrix effects, physical properties and geometry of the sample throughout the core (e.g. Tjallingii *et al.*, 2007). The easiest and most convenient way to eliminate such specimen effects is by using log-ratios of two elements, which are linear functions of log-ratios of element concentrations (Weltje and Tjallingii, 2008). Additionally, the log-ratio transformation of element intensities resolves many difficulties associated with closed-sum data that inhibit rigorous multivariate statistical analyses. The precise correlation between the composite profiles MFM6 and MFM09 based on

well-defined marker layers (Martín-Puertas *et al.*, 2012b) allowed us to transfer the μ -XRF data on to the age scale though the age–depth model performed for the sedimentary profile (Table 1; Fig. 2).

Statistically robust clustering analysis allows for objective compositional classification without prior knowledge. The Ward's hierarchical clustering analysis was applied on the complete set of XRF measurements of MFM09 ($n = 5635$) after centred log-ratio (*clr*) transformation (e.g. Aitchison, 1982) of the μ -XRF scanning data following:

$$clr I_{ij} = \ln(I_{ij}/gm_j). \quad (1)$$

Here, I_{ij} is the element intensity of element i in measurement j and gm_j is the geometric mean of all elements analysed at measurement j . Hierarchical clustering results are typically presented by a dendrogram with the number of clusters versus the Euclidian linking-distances between the clusters. As the number of clusters increases, the linking distances decrease, due to a reduction of the statistical differences. The objective of the Ward's hierarchical clustering analysis is to obtain a minimum number of clusters that provides a satisfactory description of the studied sediments. More details on the compositional differences of the individual clusters were obtained from biplots, which visualize the loadings (variables) of the principal component analyses (PCAs).

Results

Chronology

The MFM sediments are varved for most of the Holocene and Lateglacial. A floating varve chronology extending from ca. 1500 back to 14 200 cal a BP was established and anchored to an 'absolute' time scale using the Ulmener Maar Tephra (UMT) isochrones dated at $11\,000 \pm 110$ cal a BP in Lake Holzmaar sediments (Zolitschka *et al.*, 2000) as isochrone (Brauer *et al.*, 2000). This chronology is supported by ^{14}C dates on terrestrial plant macrofossil remains and published as 'MFM2000 chronology' (Brauer *et al.*, 2000). Varve interpolation was applied where varves are not preserved (dashed line in Fig. 2). Major interpolated interval occurs at the YD/Holocene boundary, where 52 varves were interpolated along 6 cm of poor varve preservation between 11 640 and 11 590 varve a BP (marker layer YD, Table 1), and at 9670 varve a BP (40 varves below marker layer K644, Table 1) 240 years was included in the chronology to fill the gap of a hiatus (see details in Brauer *et al.*, 2000). The MFM2000 has been updated and published as 'MFM2012

Table 1. Description of the marker layer used to transfer the MFM2000 chronology (MFM6) to the MFM09 profile, where μ -XRF data were measured.

Marker layer	Description	Scale of identification	Age (varve a BP)	MFM6 depth (cm)	MFM09 depth (cm)
KL8	Detrital layer	Macroscopic	9340	627.5	647
K632	Detrital layer	Microscopic	9432	632.5	652
K640	Detrital layer	Microscopic	9581	638	658
K644	Detrital layer	Microscopic	9677	644	663
K652	Thick organic layer	Microscopic	10 168	653.5	673
KL9	Detrital layer	Macroscopic	10 632	666	686
UMT	Tephra layer	Microscopic	11 000	691	711
K9	Detrital layer	Microscopic	11 223	701	721.5
15A	Detrital layer	Microscopic	11 416	713	735.2
YD	Non-varved/varved sediment transition	Macroscopic	11 584	726	750.7

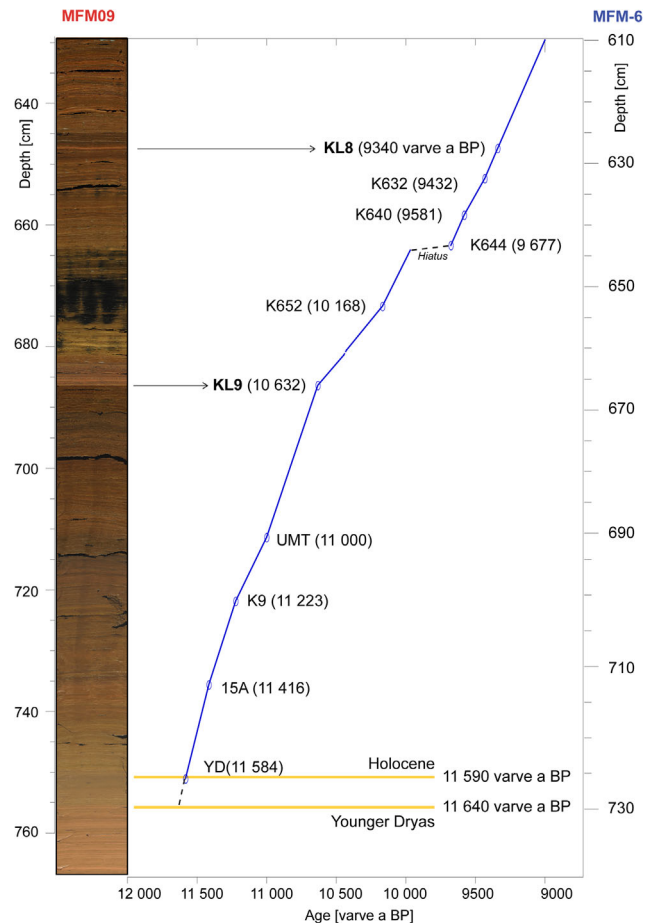


Figure 2. MFM2000 chronology for the early Holocene sequence in Lake Meerfelder Maar. Age–depth model for both profile MFM09 and MFM6, as well as marker layers used for correlation. Depth scale of the corresponding sediment sequence in MFM09 (left) and MFM6 (right). Depths in all figures and main text refer to the MFM09 composite profile. Dashed lines indicate varve interpolation.

chronology’ (Martín-Puertas *et al.*, 2012b). Re-counting on the new MFM09 composite profile was carried out for the interval between marker layers KL7 and KL1 (7796–2058 varve a BP). Comparison between the MFM2012 and MFM2000 chronologies along this interval (5738 varves) reveals counting deviations of <0.5% (29 varves), thus confirming the MFM2000 count. In this paper, we use the MFM2000 chronology for the study interval (11640–9000 varve a BP), which has been transferred in the MFM09 composite profile using macro- and microscopic marker layers (Table 1; Fig. 2).

Microfacies analyses

The Early Holocene sediments of MFM have been broadly identified as organic-diatomaceous varves with varying amount of detrital matter and irregularly intercalated distinct graded detrital layers (Fig. 3). Two different organic varve facies are distinguished. Organic varve facies 1 represents varves formed by couplets of spring/summer sub-layers made up of one or two different monospecific planktonic diatom blooms of *Stephanodiscus* sp. and/or *Cyclotella* sp., and autumn/winter sub-layers composed of organic detritus, reworked littoral diatoms and detrital silt and clays (Fig. 3b, c). Varve thickness varies between 0.24 and 3.2 mm. Organic varve facies 2 shows thinner varves (0.2 mm) formed by triplets of diatom bloom, endogenic calcite, and amorphous and particulate organic detritus sub-layers, where the

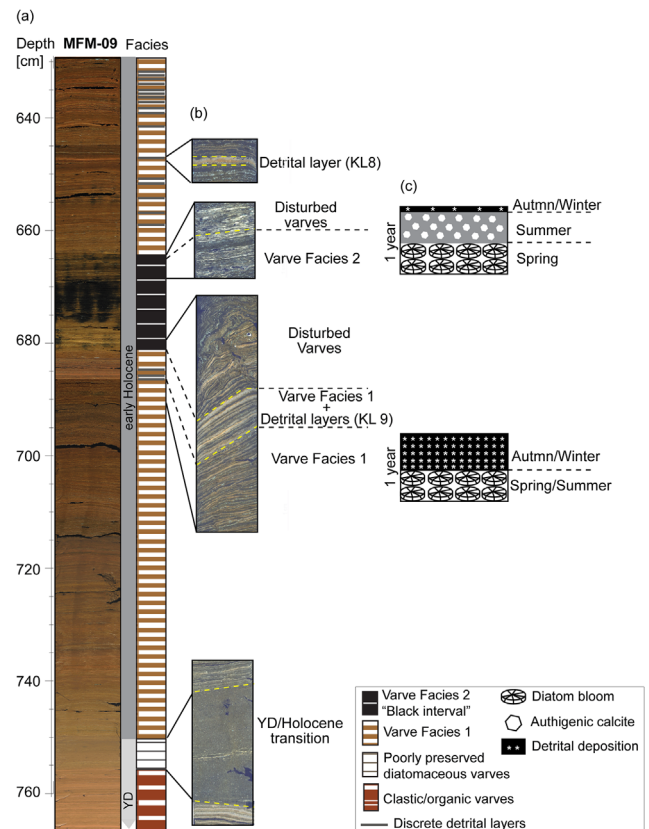


Figure 3. Early Holocene sediment sequence of Lake Meerfelder Maar (MFM09). (a) Core photo and lithological description; (b) polarized light micrographs of thin sections; (c) schema of the varve structure (seasonality) corresponding to the main varve facies described in the text.

minerogenic content is low (Fig. 3b,c). Additionally, early diagenetic (vivianite, pyrite) and syndimentary (siderite) iron-rich minerals are common throughout the cores, commonly dispersed within the sediments (Brauer *et al.*, 2000; Martín-Puertas *et al.*, 2012b).

The later half of the YD (below 756 cm) is characterized by a different varve facies, i.e. clastic–organic varves with a graded silt layer at the base of each varve (Brauer *et al.*, 1999; Lücke and Brauer, 2004). The onset of the Holocene is marked by the change in sedimentation from clastic–organic varves to predominantly organic varves (couplets, organic varve facies 1) separated by a short (4 cm) interval of poor varve preservation at the transition (756–750 cm; 11640–11590 varve a BP) (Fig. 3). Well-preserved organic varve facies 1 is temporarily replaced by the organic varve facies 2 between 664 and 682 cm depth (10530 and 9655 varve a BP), which is a 21-cm-thick interval of organic-rich sediment with occasional calcite layers and where detrital sublayers are thinner or are not present. We have labelled this episode as ‘black interval’ because of the dark appearance of the sediment core at this position (Figs 2 and 3), which makes varves undetectable by eye. Microscopically visible slump deposits (disturbed varves) appear in a 3-cm section at the bottom of this interval (682–679 cm), where 26 varves were interpolated (Figs 2 and 3b). At the top of the black interval (664 cm), a 1.5-cm-thick micro-disturbance followed by an abrupt facies change indicates the presence of the hiatus mentioned above (Brauer *et al.*, 2000; Fig. 3b).

Five intervals of thicker varves (mean thickness >0.46 mm) have been identified: 11590–11540 varve a BP (0.95 mm), 11230–11165 varve a BP (0.7 mm), 10690–10610 varve

a BP (0.77 mm), 9480–9340 varve a BP (0.56 mm) and 9300–9035 varve a BP (0.54 mm). Discrete graded, reddish detrital layers occur more frequently just before the black interval at 10650 varve a BP and in the sediment section deposited after 9655 varve a BP (Fig. 3b).

μ -XRF core scanning

Intervals with similar geochemical compositions were established statistically using Ward's hierarchical clustering analysis of the *clr*-transformed μ -XRF data. Hierarchical clustering results are typically represented as a hierarchical dendrogram of minimum variance linking distances and assigning each individual data point to one of the statistical clusters (Fig. 4a). As such, showing clustering results stratigraphically down-core can be used to objectively identify different compositional intervals (Fig. 5g). A solution with six clusters was selected based on the relative linking distances (Fig. 4) together with the match between the cluster stratigraphy, core description and microfacies analyses (Fig. 5a). Statistical results are influenced by the number of data points in a cluster and tend to reflect more general compositional changes. Matching solutions with more than six clusters would exceed the variations acquired by core observations and microfacies analyses.

The six clusters differentiate compositional changes based on the simultaneous variations of all elements acquired with μ -XRF core scanning. These compositional changes are visualized using covariance biplots of the PCA loadings of the first two principal components (Fig. 4b). Positively correlated elements will have a similar orientation in the biplot, whereas negatively correlated elements are located opposite each other. The six clusters reveal similar groups of elements (Fig. 4), which are indicative of detrital sediments (Ti, K and partly Si), diatom silica (Si), calcite (Ca) and redox-sensitive elements (Mn and Fe). Iron is predominantly linked to the presence

of vivianite, siderite and pyrite that form under reducing conditions (Brauer *et al.*, 2000). Therefore, all clusters indicate that Fe is poorly or even negatively correlated with the detrital elements, suggesting partly or completely diagenetic reduction of the original iron-bearing minerals from volcanic country rocks, which allows the use of Fe as a redox proxy (Fig. 4b).

Cluster 1 ($n=709$) reveals a good correlation of the detrital elements and Si (Fig. 4b), indicating that diatom silica plays only a minor role in these sediments. The occurrence of cluster 1 in the stratigraphic sediment column coincides with high values of Ti_{clr} , thus representing minerogenic-rich sediments. In contrast, clusters 4 ($n=1300$), 5 ($n=759$) and 6 ($n=159$) show a clear negative correlation between the detrital elements and Si, probably indicating distinct diatom bloom layers. Additionally, clusters 5 and 6 are influenced by calcium-bearing sediments, as indicated by increased $\ln(Ca/Ti)$ ratios (Fig. 5). In contrast, cluster 3 ($n=1753$) shows an influence solely of Ca variability (Fig. 4), but this is not related to an increasing abundance of Ca as shown by low $\ln(Ca/Ti)$ ratios. The latter is further supported by microfacies analyses as no major contribution of calcium-rich minerals has been observed. Clusters 2 ($n=368$) and 3 show an intermediate situation in which the detrital elements and Si are decoupled, revealing a less clear division between the deposition of the detrital and diatom sub-layers, probably because of partly overlapping or mixed sub-layers. Regarding the redox-sensitive elements, Fe and Mn are positively correlated in clusters 3, 5 and 6, while they are not correlated in clusters 1 and 4. The stratigraphic distribution of the major clusters allows us to objectively distinguish six geochemical boundaries at 11 555, 11 230, 10 650, 10 515 and 9670 varve a BP (Fig. 5g).

During the early Holocene until 5000 varve a BP, varve thickness is primarily controlled by the deposition of detrital sediments (thickness of the autumn/winter sub-layer)

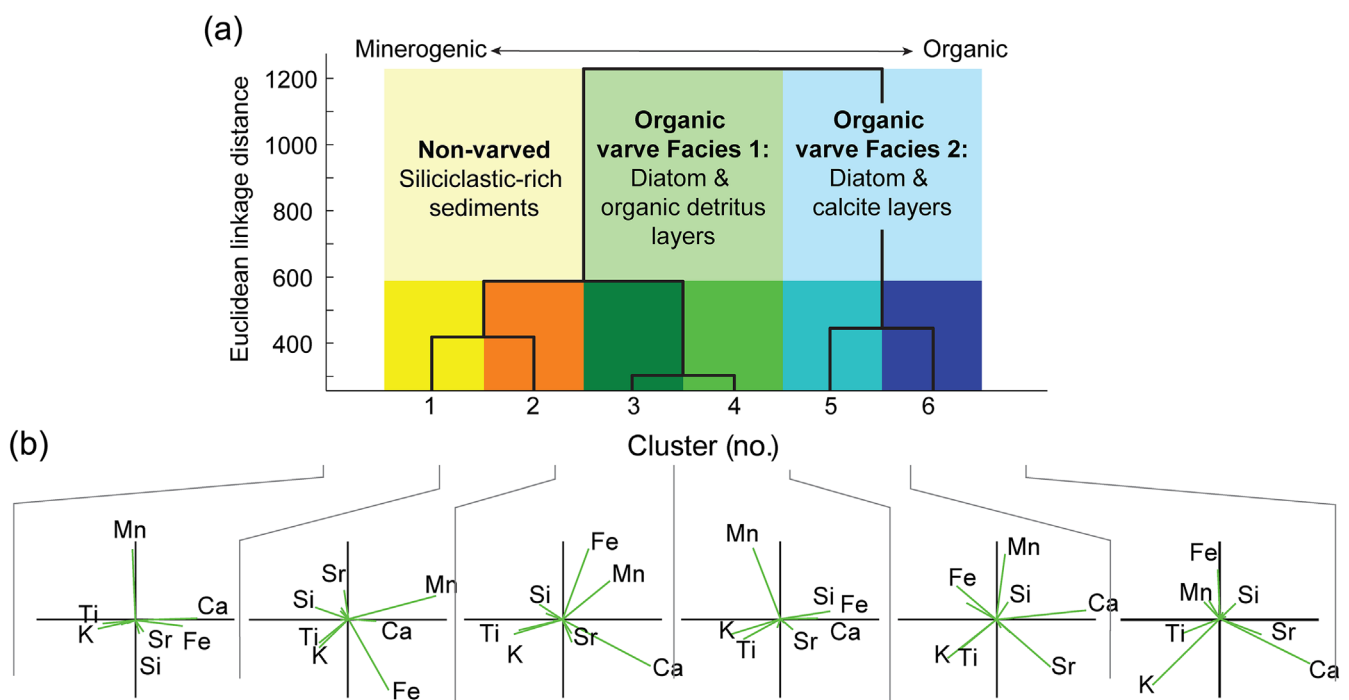


Figure 4. Hierarchical clustering results performed on the total μ -XRF core scanning data set. (a) Clustering of the μ -XRF data provides objectively defined and statistically significant sub-composition of the sediments. (b) Covariance biplot results of all individual clusters that visualize the correlation of main elements with respect to the first two principal components. The sub-compositions defined by the six-cluster solution matches with the sedimentological changes shown in Fig. 5.

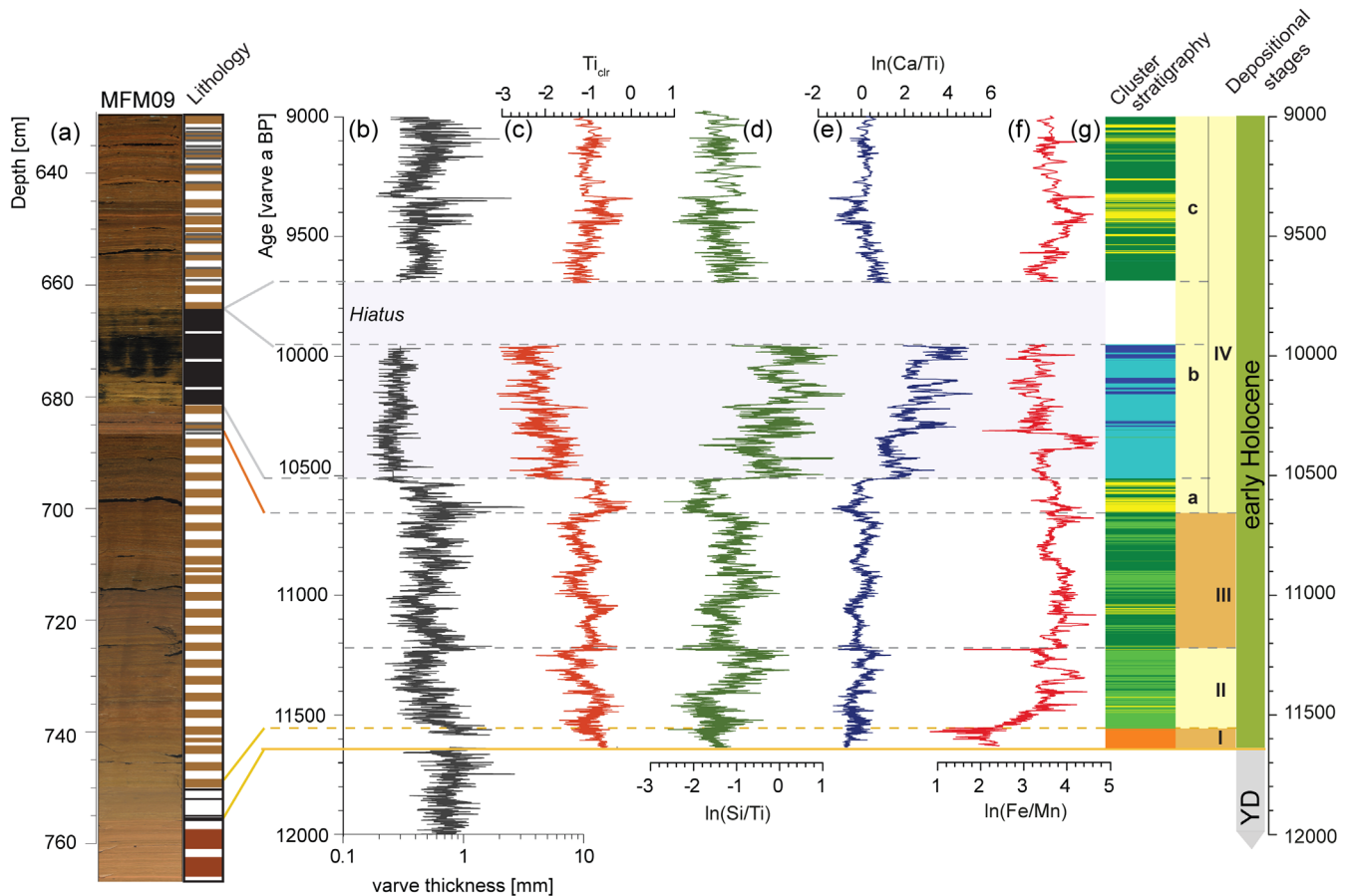


Figure 5. Environmental proxies from the early Holocene sediments of Lake Meerfelder Maar. On the depth scale: (a) core photo and lithology. On the age scale: (b) varve thickness as an indicator for sedimentation rate mainly controlled by detrital input into the lake; (c) centred-log ratio results of titanium (Ti_{clr}) as an indicator of relative changes of the bulk detrital matter; (d–f) results of $\ln(Si/Ti)$, $\ln(Ca/Ti)$ and $\ln(Fe/Mn)$ indicating relative changes of biogenic silica concentrations, authigenic calcite precipitation and oxygenation at the bottom water, respectively; and (g) cluster stratigraphy with the downcore representation of the six clusters obtained from μ -XRF core scanning data and early Holocene depositional stages defined by the clustering results and microfacies observations.

(Martín-Puertas *et al.*, 2012b) except for the aforementioned 'black interval'. Accordingly, relative variations of the varve thickness resemble the variability of Ti_{clr} (Fig. 5b,c), which is considered a proxy for minerogenic components because of the basaltic composition of the catchment (Martín-Puertas *et al.*, 2012b). Variations of diatom abundances as inferred from microfacies analyses (spring/summer sub-layer) correspond well to variations of detrital-normalized silica represented by $\ln(Si/Ti)$ ratios (Martín-Puertas *et al.*, 2012b). However, the detailed $\ln(Si/Ti)$ record suggests that diatom deposition has no substantial influence on the variations of total varve thickness (Fig. 5b,d). The exceptional 'black interval' is characterized by lowest sedimentation rates, as well as very low contents of detrital matter as indicated by low Ti_{clr} , whereas higher $\ln(Si/Ti)$ and $\ln(Ca/Ti)$ ratios reveal an increase in the relative concentrations of diatom silica and calcite, respectively (Fig. 5c–e). This supports thin-section observations of triplets of spring/summer diatom blooms followed by an endogenic calcite sub-layer and thin laminae of amorphous and particulate organic detritus (organic varve facies 2, Fig. 3c). An abrupt increase in the $\ln(Fe/Mn)$ ratio at 756 cm distinguishes YD sediments (low ratios) from Holocene sediments (high ratios) (Fig. 5a,f).

Discussion

Depositional stages

High-resolution μ -XRF core scanning data in combination with microfacies analyses allow determination of changes in

depositional environments in terms of sediment sources and sediment formation mechanisms. Hierarchical clustering of the μ -XRF core scanning data provides a tool to investigate changes of a comprehensive set of elements simultaneously. This allows identification of compositional changes of elements that are not constrained to a single mineral phase. Consequently, we use geochemically defined boundaries based on the clustering results and microfacies observations to discuss the major depositional stages in the MFM record (Fig. 5).

Depositional stage I (11 640–11 555 varve a BP) comprises the 4-cm interval of poor clastic varve preservation at the biostratigraphically defined YD–Holocene transition (Brauer *et al.*, 1999; Litt and Stebich, 1999) and also includes the first 3 cm of Holocene organic varves (Fig. 5). This stage is characterized by cluster 2 (orange), which shows a decoupling of the Si from the detrital elements Ti and K (Fig. 4). This suggests a clear separation between the deposition of detrital material and a diatom layer, indicating the formation of seasonal couplets (although in parts poorly preserved) and hence supporting varve interpolation along the first 4 cm of stage I (Figs 2 and 5b). Additionally, the boundary between stages I and II is marked by a sudden increase in the $\ln(Fe/Mn)$ ratios (Fig. 5g) reflecting a change to strengthened diagenetic processes and more anoxic bottom water conditions in the early Holocene. The sediments in this interval are further characterized by increasing organic contents.

Depositional stage II (11 590–11 230 varve a BP) is mainly represented by cluster 4 (light green) and followed by stage III

(11 230–10 650 varve a BP) that is characterized by alternations of cluster 3 (dark green) and 4 (Fig. 5) and continuous sedimentation of organic varve facies 1 (couplets). The compositional differences between cluster 3 and cluster 4 are not easily detectable by microfacies observations. Cluster 3 corresponds to thicker varves with a predominant detrital sub-layer suggesting a higher detrital input (runoff) into the lake. The biplots also show different element correlations for clusters 3 and 4 (Fig. 4b). The most distinct difference appears from the correlation between Si and detrital elements Ti and K, which is slightly positive for cluster 3 but negative for cluster 4. Also, the positive correlation of the redox-sensitive elements Fe and Mn in cluster 3 is not apparent in cluster 4. These differences suggest a less strict separation of the siliciclastic and diatom sub-layers and stronger redox conditions in *stage III*, where cluster 3 is predominant. Changes in the separation between the siliciclastic and diatom sub-layers could be explained by changing seasonality as an additional late summer bloom partly overlaps with the autumn/winter layer composed of detrital and resuspended material. Diatom assemblages of the MFM sediments show high variability in both the genus of diatoms (species have not been specified) and the number of diatom blooms, i.e. varves with only one bloom of either *Stephanodiscus* sp. or *Cyclotella* sp., and varves with two blooms (*Stephanodiscus* sp. and *Cyclotella* sp.) (Martín-Puertas *et al.*, 2012b). Alternatively, the less strict separation between siliciclastic and diatom sub-layers might also be caused by resuspension of sediments from the littoral zone comprising epiphytic diatoms during autumn as observed by microfacies analyses. Interpretation of the loading of Ca in cluster 3 (Fig. 4) remains elusive because calcium-bearing minerals are too sparse to be detected even by microscopic analyses. This is supported by the absence of significant occurrences of calcium-bearing minerals as derived from thin section analyses, which prevent us from providing a credible explanation for the Ca eigenvector in cluster 3.

The boundary between depositional *stage III* and *stage IVa* occurred at 10 650 varve a BP. *Stage IVa* is characterized by the deposition of four thicker (1–3 mm) discrete graded detrital layers (Fig. 3b) intercalated within the organic varve facies 1 and dominated by clusters 3 and 4 (Fig. 5). The detrital layers occurring in depositional *stage IVa* coincide with cluster 1 (yellow, Fig. 5g), which is characterized by the positive correlation of Si and the detrital elements Ti and K (Fig. 4b), demonstrating the siliciclastic nature of these event layers. As such, sediments related to cluster 1 and identified as discrete graded detrital layers are interpreted as surface runoff events. These events are probably triggered by heavy rainfall and/or flood events and occur more often after 10 650 varve a BP.

Depositional *stage IVb* (10 515–9670 varve a BP) reflects the 'black interval' (Fig. 5). As mentioned above, this episode is easily recognizable in the sediment sequence, even by eye. The boundaries at the bottom and the top are characterized by ~20 disturbed varves each, with an assumed hiatus of 240 years at the top (Brauer *et al.*, 2000). Varve deformations show a fold structure suggesting micro slumps that caused the hiatus at the end of *stage IVb* (Fig. 3b). Clusters 5 and 6 (light and dark blue) represent the sediments deposited during *stage IVb* (Figs 5g and 5), which differ considerably from the other early Holocene sediments. The most significant features of this stage are the strongly reduced detrital supply to the lake (low values of Ti_{clr} ; Fig. 5b,c) resulting in very low mean varve thickness of 0.2 mm, as well as the formation of annual triplets (organic varve facies 2). The biplots corresponding to

clusters 5 and 6 reveal a negative correlation between Ti and Si (Fig. 4) that is most likely due to the occurrence of seasonal diatom blooms. Also, both clusters show that Ca is decoupled from the detrital elements Ti and K, suggesting that Ca reflects endogenic calcite (Fig. 4). The difference between cluster 6 and 5 may correspond to higher values of the $\ln(Ca/Ti)$ ratio and thicker calcite layers in cluster 6, while cluster 5 represents sediments with lower Ca values and thinner calcite varves during *stage IVb* (Fig. 5). Calcite varves are exceptional in the MFM sediments and occur only within the *stage IVb* and a short interval in the Allerød (Engels *et al.*, 2016). Calcite precipitation in mid-latitude lakes is mainly induced by either seasonal increases in the photosynthetic uptake of CO_2 and/or periodic calcite supersaturation due to increasing water temperature following spring mixing (Kelts and Hsü, 1978). Primary productivity during *stage IVb*, however, is not as strong as during other intervals where calcite did not precipitate, e.g. during the 2.8-ka climatic oscillation (Martín-Puertas *et al.*, 2012a). Therefore, an alternative explanation for the formation and preservation of calcite varves in this interval might be an increased flux of Ca^{2+} through groundwater input. Periods of elevated groundwater discharges into MFM have been reported during the early Holocene (Schettler *et al.*, 1999). The most significant and prolonged peak in groundwater discharge (D2 in Schettler *et al.*, 1999) coincides well with our *stage IVb*, which supports our interpretation (Supporting Information, Fig. S1).

Stage IVb represents a unique episode in the history of the lake MFM intercalated within the continuous deposition of organic varve facies 1 (couplets), which characterizes the entire MFM sediment record during the Holocene as a whole (Brauer *et al.*, 2000; Martín-Puertas *et al.*, 2012b). Following this depositional stage, the sediments are again characterized by organic varve facies 1 and episodic flood events (*stage IVc*), which coincide with clusters 3 and 1, respectively (Fig. 5).

Sediment responses to catchment evolution and climatic change

To evaluate the possible influence of the catchment and/or climate on the evolution of the lake, the geochemically defined stages and Ti_{clr} (runoff proxy) are compared to (i) the early Holocene pollen record from MFM, as an indicator of vegetation cover and catchment stability; and (ii) the temperature-sensitive $\delta^{18}O_{ice}$ Greenland ice core record (Rasmussen *et al.*, 2006), as a sensitive recorder of climatic oscillations in the North Atlantic region (Fig. 6).

The MFM pollen record reflects the major biostratigraphic boundaries defined in northern and central Europe, i.e. the YD/Holocene transition and the Preboreal/Boreal transition (Litt and Stebich, 1999). The non-varved interval included in the depositional *stage I* coincides with a peak in *Juniperus* pollen, indicating climatic amelioration already by the final stage of the YD (Brauer *et al.*, 1999). Varves deposited before *stage I* (mainly YD sediments) have graded silt layers at their base and have been interpreted as snowmelt deposits (Brauer *et al.*, 1999). The Pleistocene–Holocene boundary as defined in the North-GRIP ice core (Walker *et al.*, 2009) (Fig. 6) falls within our *stage I* within dating uncertainties. The onset of the Holocene as defined by biostratigraphy in MFM marks the rapid reforestation with the Preboreal birch forest (*Betula*) (Litt and Stebich, 1999) and coincides with the end of the non-varved interval within *stage I*. The sediment composition apparently responds with a short delay of a few decades compared to the vegetation change. *Stage I* lasts until 11 555

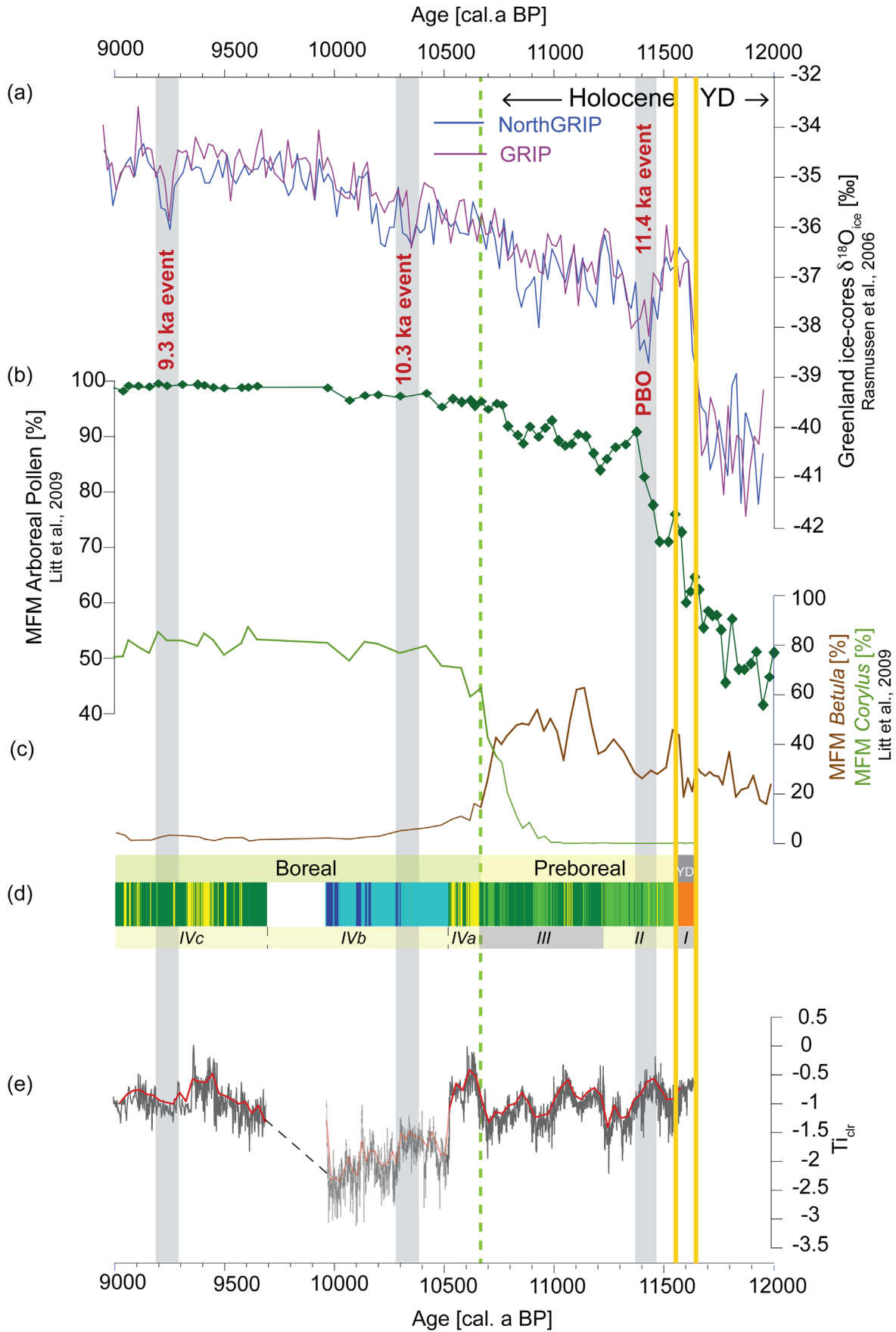


Figure 6. Regional comparison of high-resolution proxy records from Greenland and Meerfelder Maar during the early Holocene. (a) $\delta^{18}\text{O}_{\text{ice}}$ records from the Greenland ice cores GRIP and NorthGRIP, both based on the GICC05 timescale (Rasmussen *et al.*, 2006, Rasmussen *et al.*, 2014); (b,c) pollen percentages from the MFM record (Litt *et al.*, 2009); (d) stratigraphic representation of the six statistical clusters identified in the MFM sediments and depositional stages defined; (e) centred/log ratio results of titanium (Ti_{clr} , brown) and the 30-year running average (black) indicating relative changes of the bulk detrital matter.

varve a BP and includes the first 3 cm of ca. 35 organic-clastic varves after the biostratigraphic transition. That difference in the abruptness of the response of the sediment facies can be explained by the period until the vegetation was dense enough to reduce surface runoff and detrital material flux.

The Preboreal/Boreal transition is marked by a pronounced *Corylus* expansion, which reaches a maximum peak of >80% in the pollen diagram at 10700–10650 varve a BP in the MFM region (Litt *et al.*, 2009). Interestingly, the start of the *Corylus* increase coincides with the onset of stage IVa at 10650 varve a BP (Fig. 6), suggesting a close relationship between vegetation cover in the catchment and sedimentation processes. Theuerkauf *et al.* (2014) suggest that the *Corylus* expansion in Europe was favoured by increasing wetness. This is supported by our data inferring the deposition of allochthonous runoff-triggered deposits during stages IVa and IVc (cluster 1, yellow).

Unlike the depositional changes mentioned above, the boundaries that define stage IVb, which occurred abruptly, do not have an equivalent signal in regional vegetation (Fig. 6). Local environmental thresholds, probably related to hydrological conditions, are considered essential for these changes in the depositional system since the most significant features of stage IVb are the lack of detrital (river) input and the formation of calcite varves (Fig. 5). Detrital supply into MFM predominantly originates from sediment discharge by the Meerbach stream that enters the crater in the south (Fig. 1). A possible explanation for the very low abundance of detrital matter in stage IVb is an increasing lake level causing flooding of the southern part of the crater, which would have created a large shallow southern bay to the lake (Brauer *et al.*, 1999). Such a shallow bay (Fig. 1) should have acted as efficient trap for allochthonous detrital sediment influx. The strong decrease or even lack of detrital input to the deeper part of the lake suggests that flooding of the southern part of the crater probably reached a critical level between 10530 and 9655 varve a BP. A rapid lake level increase at the onset and decrease at the end of stage IVb even might have triggered the deposition of small-scale slump deposits in the deepest part of the lake since instable shorelines favoured avulsion from the littoral zone (Fig. 3b).

In contrast to the sedimentation changes related to vegetation during the early Holocene environmental amelioration, we do not find clear reflections of short cold events identified in the Greenland ice cores at 11.4 ka b2k (PBO), 10.3 ka b2k and 9.3 ka b2k in the MFM sedimentary record (Fig. 6). The absence of a sediment response, especially to the PBO, has been also reported from other lake sediments in northern and central-eastern Europe (Björck *et al.*, 1997; Ott *et al.*, 2016). One explanation for the absence of a sediment response in MFM to the PBO is that this fluctuation occurred during the strongest increase in tree pollen at the onset of the Holocene (Fig. 6), which might have superimposed environmental impacts of the climatic oscillation. The weaker climate oscillations at 10.3 and 9.3 ka b2k occurred during rather stable phases at MFM with dense *Corylus* cover in the catchment, which probably made the lake system resilient to these climate fluctuations.

Conclusions

We have demonstrated a multivariate statistical approach for the total μ -XRF core scanning dataset as a suitable tool to complement microfacies analyses and to improve the interpretation of varved sediments. This approach allows linking compositional changes obtained by μ -XRF core scanning to micro-facies proxies to better identify mechanisms controlling

the lake's depositional processes. In particular, our study on the MFM sediments confirms:

1. The lake was sensitive to surface conditions in the catchment as controlled by long-term vegetation reorganization and probably soil formation during the early Holocene.
2. The lake sedimentation reacted abruptly to major biostratigraphic transitions in the early Holocene, i.e. the YD/Holocene and the Preboreal/Boreal transition.
3. Hydrological thresholds promoted unprecedented conditions in the lake from 10 515 to 9670 varve a BP, characterized by a strong reduction of detrital supply to the deeper part of the lake and the precipitation of calcite.
4. We found no clear sediment responses to short-term early Holocene climatic oscillations because of either superimposed major changes in vegetation or stable catchment conditions.

Acknowledgements. This study was funded by the GFZ German Research Centre for Geosciences, Potsdam, Germany, and is a contribution to the Helmholtz Association climate initiative REKLIM (Topic 8 'Rapid Climate Change from Proxy data') and supported by infrastructure of the Terrestrial Environmental Observatories network (TERENO) financed by the Helmholtz Association. We thank Agathe Deriot and Nadine Walikewtz for their contribution to varve counting, Gert Jan Weltje for the extensive discussion of multivariate analyses of μ -XRF scanning data, Georg Schettler for providing the data shown in Fig. S1, Andreas Hendrich for support with graphics, Dieter Berger and Gabi Arnold for technical support with thin section preparation, and Brian Brademann and the coring team for recovering excellent cores. We also thank Professor Geoff Duller and two anonymous referees for valuable comments on the manuscript.

Supporting Information

Figure S1. Groundwater discharges in the Lake Meerfelder Maar. Transference of the MFM2000 chronology to the composite profiles MFM 2a–2b (Schettler *et al.*, 1999) via correlation with the percentage of total organic carbon (TOC). From bottom to top: U/Be ratio and percentage of TOC from the composite profile MFM 2a–2b published by Schettler *et al.* (1999); percentage of TOC and age–depth model for the composite profile MFM6. D1–D3 indicate positive groundwater discharge (Schettler *et al.*, 1999). UMT: Ulmener Tephra Layer (11 000 varve a BP).

Abbreviations. BO, Boreal Oscillation; *clr*, centred log-ratio; MFM, Lake Meerfelder Maar; μ -XRF, micro X-ray fluorescence; PBO, Preboreal Oscillation; PCA, principal components analysis; UMT, Ulmener Maar Tephra; YD, Younger Dryas.

References

- Aitchison J. 1982. The statistical analysis of compositional data. *Journal of the Royal Statistical Society. Series B: Statistical Methodology* **44**: 139–177.
- Björck S, Rundgren M, Ingólfsson O *et al.* 1997. The Preboreal oscillation around the Nordic Seas: terrestrial and lacustrine responses. *Journal of Quaternary Science* **12**: 455–465.
- Björck S. 2008. The late Quaternary development of the Baltic Sea basin. In *Assessment of climate change for the Baltic Sea Basin*, the BACC Author Team (eds). Springer-Verlag: Berlin Heidelberg; 398–407.
- Bloemsma MR, Zabel M, Stuut JBW *et al.* 2012. Modelling the joint variability of grain size and chemical composition in sediments. *Sedimentary Geology* **280**: 135–148.
- Bos JAA, van Geel B, van der Plicht J *et al.* 2007. Preboreal climate oscillations in Europe: wiggle-match dating and synthesis of Dutch high-resolution multi-proxy records. *Quaternary Science Reviews* **26**: 1927–1950 [doi:10.1016/j.quascirev.2006.09.012].

- Brauer A, Endres C, Günter C *et al.* 1999. High resolution sediment and vegetation responses to Younger Dryas climate change in varved lake sediments from Meerfelder Maar, Germany. *Quaternary Science Reviews* **18**: 321–329 [doi:10.1016/S0277-3791(98)00084-5].
- Brauer A, Endres C, Zolitschka B *et al.* 2000. AMS radiocarbon and varve chronology from the annually laminated sediment record of Lake Meerfelder Maar, Germany. *Radiocarbon* **42**: 355–368 [doi:10.1017/S0033822200030307].
- Czymzik M, Brauer A, Dulski D *et al.* 2013. Orbital and solar forcing of shifts in Mid- to Late Holocene flood intensity from varved sediments of pre-alpine Lake Ammersee (southern Germany). *Quaternary Science Reviews* **61**: 96–110. [doi:10.1016/j.quascir.2012.11.010]
- Dulski P, Brauer A, Mangili C. 2015. Combined μ -XRF and microfacies techniques for lake sediment analysis. In *Developments in Paleoenviromental Research, Micro-XRF Studies of Sediment Cores, Applications of a Non-destructive Tool for the Environmental Sciences*, Croudace IW, Rothwell RG (eds). Springer: Dordrecht, Netherlands; 325–349.
- Engels S, Brauer A, Buddelmeijer N *et al.* 2016. Subdecadal-scale vegetation response to a previously unknown late-Allerød climate fluctuation and Younger Dryas cooling at Lake Meerfelder Maar (Germany). *Journal of Quaternary Science* **31**: 741–752 [DOI: 10.1002/jqs.2900].
- von Grafenstein U, Erlenkeuser H, Brauer A *et al.* 1999. A mid-European decadal isotope-climate record from 15,500 to 5000 years B.P. *Science* **284**: 1654–1657 [doi:10.1126/science.284.5420.1654].
- Kelts K, Hsü K. 1978. Freshwater carbonate sedimentation. In: *Lakes: Physics, Chemistry and Geology*, Lerman A (ed). Springer: New York; 295–323.
- Lauterbach S, Brauer A, Andersen N *et al.* 2011. Multi-proxy evidence for early to mid-Holocene environmental and climatic changes in northeastern Poland. *Boreas* **40**: 57–72 [doi:10.1111/j.1502-3885.2010.00159.x].
- Litt T, Schölzel C, Kühl N *et al.* 2009. Vegetation and climate history in the Westeifel Volcanic Field (Germany) during the past 11 000 years based on annually laminated lacustrine maar sediments. *Boreas* **38**: 679–690 [doi:10.1111/j.1502-3885.2009.00096.x].
- Litt T, Stebich M. 1999. Bio- and chronostratigraphy of the lateglacial in the Eifel region, Germany. *Quaternary International* **61**: 5–16. [doi:10.1016/S1040-6182(99)00013-0]
- Lücke A, Brauer A. 2004. Biogeochemical and micro-facial fingerprints of ecosystem response to rapid Late Glacial climatic changes in varved sediments of Meerfelder Maar (Germany). *Palaeo-geography, Palaeoclimatology, Palaeoecology* **211**: 139–155.
- Martín-Puertas C, Brauer A, Dulski P *et al.* 2012b. Testing climate-proxy stationarity throughout the Holocene: an example from the varved sediments of Lake Meerfelder Maar (Germany). *Quaternary Science Reviews* **58**: 56–65 [doi:10.1016/j.quascir.2012.10.023].
- Martin-Puertas C, Matthes K, Brauer A *et al.* 2012a. Regional atmospheric circulation shifts induced by a grand solar minimum. *Nature Geoscience* **5**: 397–401 [doi:10.1038/ngeo1460].
- Masson-Delmotte V, Landais A, Stievenard M *et al.* 2005. Holocene climatic changes in Greenland: different deuterium excess signals at Greenland Ice Core Project (GRIP) and NorthGRIP. *Journal of Geophysical Research: Atmospheres* **110**: D14102 [doi:10.1029/2004JD005575].
- McDermott F, Matthey DP, Hawkesworth C. 2001. Centennial-scale Holocene climate variability revealed by a high-resolution speleothem $\delta^{18}\text{O}$ record from SW Ireland. *Science* **294**: 1328–1331 [doi:10.1126/science.1063678] [PubMed:11701925].
- Negendank JFW, Brauer A, Zolitschka B. 1990. Die Eifelmaare als erdgeschichtliche Fallen und Quellen zur Rekonstruktion des Paläoenvironments. *Mainzer geowissenschaftliche Mitteilungen* **19**: 235–65.
- Ott F, Wulf S, Serb J, *et al.* 2016. Constraining the time span between the Early Holocene Håsseldalen and Askja-S Tephra through varve counting in the Lake Czechowskie sediment record, Poland. *Journal of Quaternary Science* **31**: 103–113. [doi:10.1002/jqs.2844]
- Rasmussen SO, Andersen KK, Svensson AM *et al.* 2006. A new Greenland ice core chronology for the last glacial termination. *Journal of Geophysical Research* **111**: D06102 [doi:10.1029/2005JD006079].
- Rasmussen SO, Bigler M, Blockley SP *et al.* 2014. A stratigraphic framework for abrupt climatic changes during the Last Glacial period based on three synchronized Greenland ice-core records: refining and extending the INTIMATE event stratigraphy. *Quaternary Science Reviews* **106**: 14–28. [doi:10.1016/j.quascir.2014.09.007].
- Renssen H. 2001. The climate in the Netherlands during the Younger Dryas and Preboreal: means and extremes obtained with an atmospheric general circulation model. *Geologie en Mijnbouw Netherlands Journal of Geosciences* **80**: 19–30.
- Schettler G, Rein B, Negendank JFW. 1999. Geochemical evidence for Holocene palaeodischarge variations in lacustrine records from the Westeifel Volcanic Field, Germany: Schalkenmehrener Maar and Meerfelder Maar. *Holocene* **9**: 381–400.
- Theuerkauf M, Bos JAA, Jahns S, *et al.* 2014. *Corylus* expansion and persistent openness in the early Holocene vegetation of northern central Europe. *Quaternary Science Reviews* **90**: 183–198 [doi:10.1016/j.quascir.2014.03.002].
- Tjallingii R, Röhl U, Kölling M *et al.* 2007. Influence of the water content on X-ray fluorescence core-scanning measurements in soft marine sediments. *Geochemistry, Geophysics, Geosystems* **8** [doi:10.1029/2006GC001393].
- Walker M, Johnsen S, Rasmussen SO *et al.* 2009. Formal definition and dating of the GSSP (Global Stratotype Section and Point) for the base of the Holocene using the Greenland NGRIP ice core, and selected auxiliary records. *Journal of Quaternary Science* **24**: 3–17 [DOI: 10.1002/jqs.1227].
- Weltje G, Tjallingii R. 2008. Calibration of XRF core scanners for quantitative geochemical logging of sediment cores: theory and application. *Earth and Planetary Science Letters* **274**: 423–438 [doi:10.1016/j.epsl.2008.07.054].
- Wohlfarth B, Lacourse T, Bennike O *et al.* 2007. Climatic and environmental changes in north-western Russia between 15,000 and 8000 calyrBP: a review. *Quaternary Science Reviews* **26**: 1871–1883 [doi:10.1016/j.quascir.2007.04.005].
- Zolitschka B, Brauer A, Negendank JFW *et al.* 2000. Annually dated Late Weichselian continental paleoclimate record from the Eifel, Germany. *Geology* **28**: 783–786 [doi:10.1130/0091-7613(2000)028<0783:ADLWCP>2.3.CO;2].